Effects of a phase transition on HBT correlations in an integrated Boltzmann + hydrodynamics approach

Qingfeng Li [a,b,*], Jan Steinheimer [c], Hannah Petersen [b,c], Marcus Bleicher [c], Horst Stöcker [b,c,d]

[a] *School of Science, Huzhou Teachers College, Huzhou 313000, China*
[b] *Frankfurt Institute for Advanced Studies (FIAS), Johann Wolfgang Goethe-Universität, Ruth-Moufang-Str. 1, D-60438 Frankfurt am Main, Germany*
[c] *Institut für Theoretische Physik, Johann Wolfgang Goethe-Universität, Max-von-Laue-Str. 1, D-60438 Frankfurt am Main, Germany*
[d] *Gesellschaft für Schwerionenforschung (GSI), Planckstr. 1, D-64291 Darmstadt, Germany*

ARTICLE INFO

ABSTRACT

A systematic study of HBT radii of pions, produced in heavy ion collisions in the intermediate energy regime (SPS), from an integrated $(3 + 1)$d Boltzmann + hydrodynamics approach is presented. The calculations in this hybrid approach, incorporating an hydrodynamic stage into the Ultra-relativistic Quantum Molecular Dynamics transport model, allow for a comparison of different equations of state retaining the same initial conditions and final freeze-out. The results are also compared to the pure cascade transport model calculations in the context of the available data. Furthermore, the effect of different treatments of the hydrodynamic freeze-out procedure on the HBT radii are investigated. It is found that the HBT radii are essentially insensitive to the details of the freeze-out prescription as long as the final hadronic interactions in the cascade are taken into account. The HBT radii R_L and R_O and the R_O/R_S ratio are sensitive to the EoS that is employed during the hydrodynamic evolution. We conclude that the increased lifetime in case of a phase transition to a QGP (via a Bag Model equation of state) is not supported by the available data.

© 2009 Elsevier B.V. All rights reserved.

1. Introduction

One of the main purposes of the research in heavy ion collisions (HICs) at high beam energies is to explore the existence of the quark gluon plasma (QGP) as well as its properties. The equation of state (EoS) of nuclear matter is one of the key points to gain further understanding since the EoS directly provides the relationship between the pressure and the energy at a given net-baryon density. Phase transitions (PT), e.g., from the hadron resonance gas phase (HG) to the color-deconfined QGP (see, e.g., [1–3]), constitute themselves in changes of the underlying EoS.

Although, on the low temperature side (and for low baryo-chemical potentials μ_B), investigations of the EoS of nuclear matter have been pursued for many years and uncertainties have been largely reduced, on the high temperature side, the EoS of hot and dense QCD matter is still not precisely known. For systems cre-

ated in the RHIC energy region with high temperatures and low baryo-chemical potential, lattice quantum chromodynamics (lQCD) (see, e.g., Ref. [4]) calculations predict a cross-over transition between the hadron gas and the QGP phase. The additional structures of the phase diagram are still under heavy debate, especially regarding the existence or non-existence of a critical endpoint [5].

The intermediate SPS energy regime still raises a lot of interest because the onset of deconfinement is expected to occur at those energies and the possibility of a critical endpoint and a first-order phase transition is not yet excluded. Several beam-energy dependent observables such as the particle ratios [6,7], the flow [8–10], the HBT parameters [11–13] show a non-monotonic behavior around $E_{\text{lab}} = 30$–$40A$ GeV and the interpretation remains still unclear. Therefore, future energy scan programs at RHIC, SPS and FAIR are planned to explore the high-μ_B region of the phase diagram in more detail.

To learn something about the hot and dense stage of the collision from the final state particle distributions, a dynamical modeling of the whole process is necessary. Some of the important ingredients which have to be considered in a consistent manner are

- the initial conditions and the initial non-equilibrium dynamics,

* Corresponding author at: Frankfurt Institute for Advanced Studies (FIAS), Johann Wolfgang Goethe-Universität, Ruth-Moufang-Str. 1, D-60438 Frankfurt am Main, Germany.

E-mail addresses: liqf@fias.uni-frankfurt.de (Q. Li), steinheimer@th.physik.uni-frankfurt.de (J. Steinheimer), petersen@th.physik.uni-frankfurt.de (H. Petersen), bleicher@th.physik.uni-frankfurt.de (M. Bleicher), h.stoecker@gsi.de (H. Stöcker).

- the treatment of the phase transition and hadronization, as well as the right degrees of freedom,
- viscosity effects in the initial partonic as well as in the hadronic stage of the evolution,
- hadronic rescatterings and freeze-out dynamics.

We notice that part of these have been pointed out to be of importance especially for the understanding of the HBT results [14–16].

Combined microscopic + macroscopic approaches are among the most successful ideas for the modeling of the bulk properties of HICs [17–19]. Recently, a transport approach that embeds a full $(3 + 1)$ dimensional ideal relativistic one fluid evolution for the hot and dense stage of the reaction has been developed and first results are convincing [20,21]. This hybrid model inherits the advantages of the Ultra-relativistic Quantum Molecular Dynamics (UrQMD) model for the dynamic treatment of the initial and the final state by taking into account event-by-event fluctuations. Furthermore, the hybrid model allows for a dynamical coupling between hydrodynamics and transport calculation in such a way that one can compare calculations with various EoS during the hydrodynamic evolution and with the pure cascade calculations within the same framework.

It is well known that by using HBT interferometry techniques one can get detailed information about the space–time configuration of the system at freeze-out. We concentrate here on the two (identical) pion interferometry and test the sensitivity of the HBT results on different stages of the evolution. In our previous investigations on the HBT correlation of various identical particle pairs from HICs at AGS, SPS, and RHIC energies [13,22–26], we adopted the UrQMD model but further considered the mean field potentials for both confined and "pre-formed" particles in the model [13,25, 26]. We found that also initial stage interaction may contribute to a better description of the HBT time-related puzzle throughout the energies from AGS, SPS, up to RHIC.

In this Letter we perform a systematic investigation of the sensitivity of HBT correlation of negatively charged pions to the EoS by applying the newly developed hybrid approach. Similar more focused studies were frequently discussed with microscopic transport or hydrodynamic models before [11,27–29]. It is also interesting to study if the current set of EoS employed in the hydrodynamic phase support the conclusion about the origin of the HBT time-related puzzle. In addition, the effects of the hadronic rescattering and of resonance decays (dubbed as "HR") after the hydrodynamic freeze-out on the HBT radii and the R_O/R_S ratio deserve more investigation. We have also noticed that some recent progresses of this topic both from an improved hydrodynamic calculation [16] and from the pion-optical-potential point of view [30] have been published which provides additional new insights.

The Letter is arranged as follows. In the next section, the UrQMD + hydrodynamics hybrid model is introduced briefly. The set of different EoS that are employed in the hydrodynamic phase are explained. Two different treatments for the transition process from the hydrodynamic evolution to the final state hadronic cascade are discussed. In Section 3, the analyzing program CRAB for constructing the HBT correlator and the corresponding three dimensional (3D) Gaussian fitting process are introduced. In Section 4, the HBT radii R_L, R_O, and R_S, and the R_O/R_S ratio of the negatively charged pion source from central Pb + Pb collisions at SPS energies are shown and discussed in the context of the experimental data. Finally, in Section 5, a summary and an outlook are given.

2. UrQMD + hydrodynamic model

An integrated Boltzmann + hydrodynamics transport approach is applied to simulate the dynamics of the heavy ion collision. To mimic experimental conditions as realistic as possible the initial conditions and the final hadronic freeze-out are calculated using the UrQMD approach. Especially for an observable like HBT radii it is important to take care of the complexity of the different effects [14,15]. The non-equilibrium dynamics, e.g. fluctuations of the local baryon and energy density [31], in the very early stage of the collision and the final state hadronic interactions are properly taken into account on an event-by-event-basis.

UrQMD is a microscopic transport approach based on the covariant propagation of constituent (anti-)quarks and diquarks accompanied by mesons and baryons, as well as the corresponding anti-particles, i.e., full baryon–anti-baryon symmetry is included. It simulates multiple interactions of ingoing and newly produced particles, the excitation and fragmentation of color strings [32–34] and the formation and decay of hadronic resonances [35,36]. In principle it is also possible to incorporate mean field interactions in the transport calculation, In the present calculation they are neglected in order to test the hydro-phase and in the following we will refer to the pure cascade calculation as UrQMD-2.3. Studies on the thermodynamic properties of UrQMD can be found in [37–39].

The coupling between the UrQMD initial state and the hydrodynamical evolution proceeds when the two Lorentz-contracted nuclei have passed through each other, $t_{start} = 2R/\sqrt{\gamma^2 - 1}$ [20]. After that, a full $(3 + 1)$ dimensional ideal hydrodynamic evolution is performed using the SHASTA algorithm [1,40]. The hydrodynamic evolution is stopped, if the energy density ε of all cells drops below five (default value) times the ground state energy density ε_0 (i.e. ~ 730 MeV/fm^3). This criterion corresponds to a T–μ_B-configuration where the phase transition is expected – approximately $T = 170$ MeV at $\mu_B = 0$. The hydrodynamic fields are then mapped to particle degrees of freedom via the Cooper–Frye equation on an isochronous (in the computational frame) hypersurface. The particle vector information is then transferred back to the UrQMD model, where rescatterings and final decays are calculated using the hadronic cascade. We will further refer to this kind of freeze-out procedure as the isochronous freeze-out (IF). This procedure is explained in detail in [21].

In this Letter we introduce another freeze-out procedure to account for the large time dilatation that occurs for fluid elements at large rapidities. Faster fluid elements need a longer time to cool down to the same temperatures than the cells at midrapidity since the hydrodynamic calculation is performed in the center-of-mass frame of the collision. At higher energies the isochronous hypersurface increasingly differs from an iso-τ hypersurface (τ is the proper time). To mimic an iso-τ hypersurface we therefore freeze out transverse slices, of thickness $\Delta z = 0.2$ fm, whenever all cells of that slice fulfill our freeze-out criterion. For each slice we apply the isochronous procedure described above separately. By doing this we obtain a rapidity independent freeze-out temperature even for the highest beam energies. For lower energies ($E_{lab} \lesssim 80A$ GeV) the two procedures yield very similar results for the temperature distributions. The hydrodynamic fields are then again mapped to particle degrees of freedom via the Cooper–Frye equation on this new hypersurface. In the following we will refer to this procedure as "gradual freeze-out" (GF). A more detailed description of the hybrid model including parameter tests and results for multiplicities and spectra can be found in [21].

Serving as an input for the hydrodynamical calculation the EoS strongly influences the dynamics of an expanding system. In this work we use three different EoS to investigate their effect on the extracted HBT radii. The first EoS, named the hadron gas (HG), describes a non-interacting gas of free hadrons [41]. Included here are all reliably known hadrons with masses up to 2 GeV, which is equivalent to the active degrees of freedom of the UrQMD model (note that this EoS does not contain any form of phase transition). This purely hadronic calculation serves as a baseline cal-
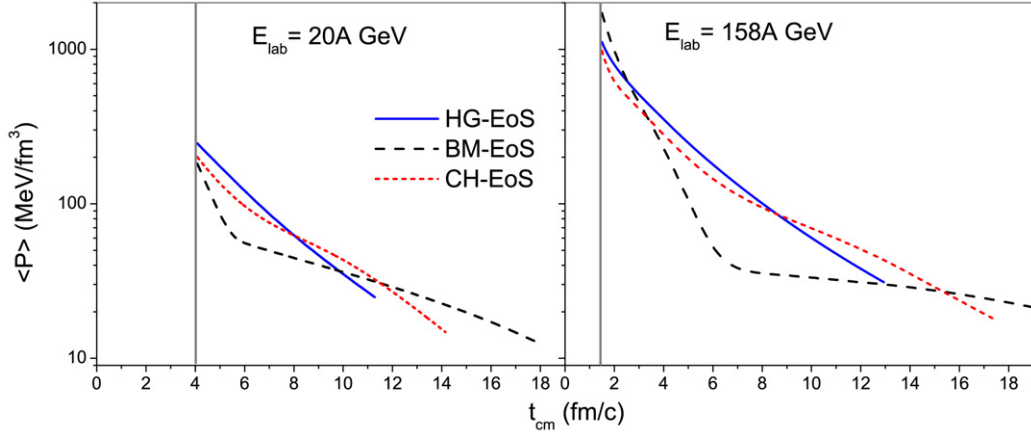
Fig. 1. Time (in the center of mass frame) evolution of the average pressure for all three EoS and a central Pb + Pb collision at $E_{lab} = 20A$ GeV (left plot) and $E_{lab} = 158A$ GeV (right plot). The vertical line in each plot indicates the starting time of the hydro evolution.

culation to explore the effects of the change in the underlying dynamics – pure transport vs. hydrodynamic calculation. The second EoS, named the Bag Model EoS (BM), follows from coupling a bag model of massless quarks and gluons to a Walecka type of hadron gas including only $SU(2)$ flavors (for details the reader is referred to [1]). This EoS exhibits a strong first-order phase transition (with large latent heat) for all baryonic chemical potentials μ_B. The third EoS, named the chiral + HG (CH), follows from a chiral hadronic $SU(3)$ Lagrangian and incorporates the complete set of baryons from the lowest flavor-$SU(3)$ octet, as well as the entire multiplets of scalar, pseudo-scalar, vector and axial-vector mesons [42]. Additional baryonic degrees of freedom are included to produce a first-order phase transition in certain regimes of the $T–\mu_q$ plane, depending on the couplings [28,43,44]. Using this EoS, a phase structure including a first-order phase transition and a critical endpoint at finite μ_B is obtained [45]. This EoS has already been successfully applied to a hydrodynamic calculation [20].

To visualize the differences of these EoS, Fig. 1 shows the average pressure of the expanding system, from central Pb + Pb collisions at $E_{lab} = 20A$ GeV (left plot) and $158A$ GeV (right plot), as a function of time (in the center of mass frame). The vertical line in each plot indicates the starting time of the hydro evolution. The mean value of the pressure has been obtained by weighting the pressure, P_i, in every cell i by its energy density, ε_i, and integrating over the hydrodynamic grid

$$\langle P \rangle = \frac{\sum_i P_i \cdot \varepsilon_i}{\sum_i \varepsilon_i}. \tag{1}$$

All curves in Fig. 1 are plotted until the point in time when the isochronous freeze-out criterion is fulfilled. Compared to the HG the BM-EoS leads to a delayed freeze-out time (i.e. a much longer expansion). While in the first few fm/c of the evolution, the system obeying the BM-EoS expands most violently (due to the high pressure gradient in the QGP phase), once the system enters the mixed phase, its expansion is slowed down considerably. This can be observed as the "kink" in Fig. 1. At the higher beam energy, $E_{lab} = 158A$ GeV, this softening of the EoS is even more pronounced. Since the HG-EoS does not contain any phase transition, no softening can be observed, resulting in the shortest expansion time. The chiral CH-EoS lies in between both extreme cases. Although a small kink can be observed, it is not as pronounced as in the BM-EoS. The effect of changes in the EoS on HBT results has been studied before [28], but the great advantages of our approach are the full $(3 + 1)$ dimensions and the same initial conditions and freeze-out for all three cases and all beam energies without adjusting additional parameters.

3. CRAB analyzing program and the fitting process

To calculate the two-particle correlator, the CRAB program is adopted [46], which is based on the formula:

$$C(\mathbf{k}, \mathbf{q}) = \frac{\int d^4 x_i \, d^4 x_j \, g(x_i, p_i) g(x_j, p_j) |\phi(\mathbf{r}', \mathbf{q}')|^2}{\int d^4 x_i \, g(x_i, p_i) \int d^4 x_j \, g(x_j, p_j)}. \tag{2}$$

Here $g(x_i, p_i)$ is an effective probability for emitting a particle i with 4-momentum $p_i = (E_i, \mathbf{p}_i)$ from the space–time point $x_i = (t_i, \mathbf{r}_i)$. $\phi(\mathbf{r}', \mathbf{q}')$ is the relative wave function with $\mathbf{r}'$ being the relative position in the pair's rest frame. $\mathbf{q} = \mathbf{p}_i - \mathbf{p}_j$ and $\mathbf{k} = (\mathbf{p}_i + \mathbf{p}_j)/2$ are the relative momentum and the average momentum of the two particles i and j.

In this work, we select central ($< 7.2\%$ of the total cross section σ_T) Pb + Pb collisions at SPS energies: $E_b = 20A$, $30A$, $40A$, $80A$ and $158A$ GeV, with a pair rapidity cut $|Y_{\pi\pi}| < 0.5$ ($Y_{\pi\pi} = \log((E_1 + E_2 + p_{\|1} + p_{\|2})/(E_1 + E_2 - p_{\|1} - p_{\|2}))/2$ is the pair rapidity with pion energies E_1 and E_2 and longitudinal momenta $p_{\|1}$ and $p_{\|2}$ in the center of mass system). For each EoS about 2500 events are calculated. All particles with their phase space coordinates at freeze-out are then given into the CRAB analyzing program. Only the negatively charged pions are considered during the analyzing process (for each analysis, one hundred million pion pairs are considered). For the cascade calculations, we take the results from our previous publications as reference [13,23]. We found that the residual Coulomb effect after the hadron freeze-out on the HBT radii of the pion source is small [25], therefore we omit it in the present analysis. Finally, we choose the longitudinal comoving system (LCMS) frame of the pair (also called the "Out-Side-Long" system), in which the longitudinal component of the pair velocity vanishes), which is frequently adopted in recent years, and fit the correlator by a 3D Gaussian distribution

$$C(q_O, q_S, q_L)$$
$$= K[1 + \lambda \exp(-R_L^2 q_L^2 - R_O^2 q_O^2 - R_S^2 q_S^2 - 2R_{OL}^2 q_O q_L)]. \tag{3}$$

Here K is the overall normalization factor, the q_x and R_x are the components of the pair relative momentum and homogeneity length (HBT radius) in the x direction, respectively. The λ parameter is called as the incoherence factor or, more correctly, the intercept parameter and lies for Bose–Einstein statistics between 0 and 1 for two-boson correlations in realistic HICs. Because the parameter λ might be influenced by many additional factors, such as contamination, long-lived resonances, or the details of the residual Coulomb modification, we regard it as a free parameter and do not show it in this Letter. However, In [25] we have found that
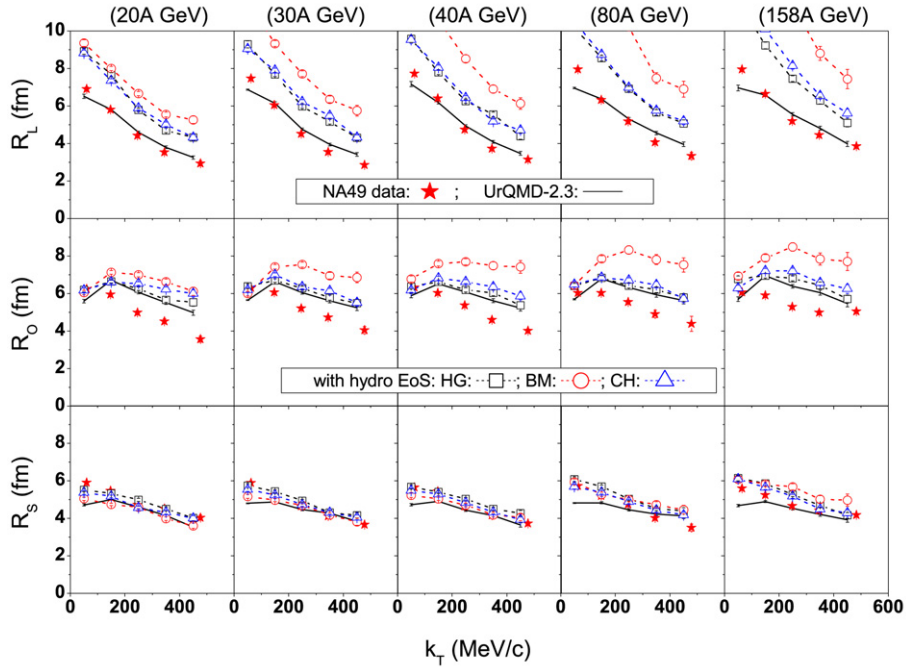
Fig. 2. Transverse momentum k_T dependence of the HBT radii R_L, R_O, and R_S (at midrapidity) of π^- source from central HICs at SPS energies ($E_{lab} = 20A$, $30A$, $40A$, $80A$, and $158A$ GeV). The NA49 data are indicated by solid stars [48]. The pure cascade calculation is depicted by lines while the hybrid model calculations with different EoS (HG, BM and CH) are depicted by dashed lines with open symbols.

the calculated λ factor with UrQMD can be comparable with experimental data at RHIC energies (although somewhat larger than data). At SPS energies, $\lambda_{\mathrm{UrQMD}} \approx 0.8$–$0.9$, is also compatible with experimental data which $\lambda_{\mathrm{data}} \approx 0.6$–$0.8$. The R_{OL}^2 represents the cross-term and plays a role at large rapidity. To fit the correlator with Eq. (3), we use ROOT [47] software and minimize χ^2.

4. HBT results

Fig. 2 shows the transverse momentum k_T ($\mathbf{k}_T = (\mathbf{p}_{1T} + \mathbf{p}_{2T})/2$) dependence of the HBT radii R_L, R_O, and R_S (at midrapidity) of π^- source from central Pb + Pb collisions at SPS energies. The data (solid stars) are from the NA49 Collaboration [48]. The pure cascade calculation is depicted by lines while the hybrid model calculations with different EoS (HG, BM and CH) are depicted by dashed lines with open symbols. As was shown before, the cascade calculation gives a fairly good result of the k_T dependence of R_L and R_S values except at quite small k_T, while for R_O, it is slightly larger than data at large k_T. In contrast, the hybrid model calculations show large HBT (for all employed EoS, but to a varying degree) in all directions, especially in the longitudinal direction. The HG and CH are moderately increased and lead to very similar results for all three directions. The large latent heat in the bag model leads to a further strong increase in the longitudinal direction and in the transverse direction at large k_T. This increase in the BM mode becomes more pronounced at higher beam energies. At first glance, this result might be surprising because at least in the transverse direction one would expect a faster expansion including a hydrodynamic evolution. On the other hand, one knows that the system spends a longer time without emitting any particles in the hybrid model calculation.

Fig. 3 exhibits the freeze-out time dependence of the π^- emission in central Pb + Pb at $E_{lab} = 20A$ GeV (left plot) and $E_{lab} = 158A$ GeV (right plot). It is clearly seen that there are almost no pions emitted before ~ 10 fm/c in the hybrid model calculations. This is easy to understand because even in the gradual hydro-
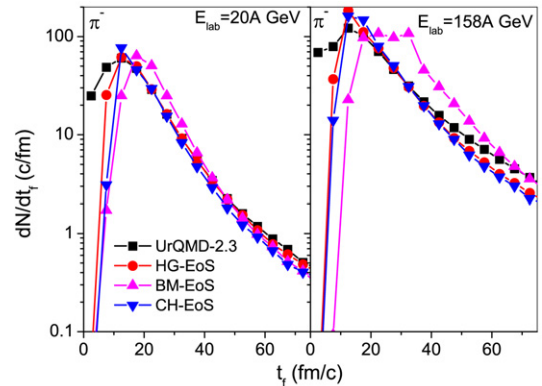

Fig. 3. Freeze-out time dependence of the π^- emission in central Pb + Pb at $E_{lab} = 20A$ GeV (left plot) and $158A$ GeV (right). Calculations with the UrQMD cascade are compared with the hybrid model calculations with the EoS of HG, BM, and CH.

freeze-out which is applied here, it takes a while until the first slices have cooled down and are frozen out from the hydrodynamic evolution. There is no particle emission from earlier times in contrast to the pure cascade calculation. For the BM-EoS, this effect is present even for a longer time since the expansion lasts longer.[1] The on-the-average longer freeze-out time leads to an apparently larger size of the pion source. Furthermore, it is clear (and expected) that the EoS with larger latent heat (such as in the BM mode) leads to a longer emission duration of the particles (as seen in Fig. 3 when $t_f \gtrsim 15$ fm/c) so that it produces larger HBT radii. This behavior is clearly seen in the more time-dependent directions R_L and R_O. This behavior might be improved by allowing particles also to freeze out and fly into the detector at all times of the collision. Especially, if there are fast pions produced during the first hard collisions in UrQMD at the edge of the system they

---

[1] This might change, if a continuous emission approach is used for the hydrodynamic model e.g. suggested in [49,50].
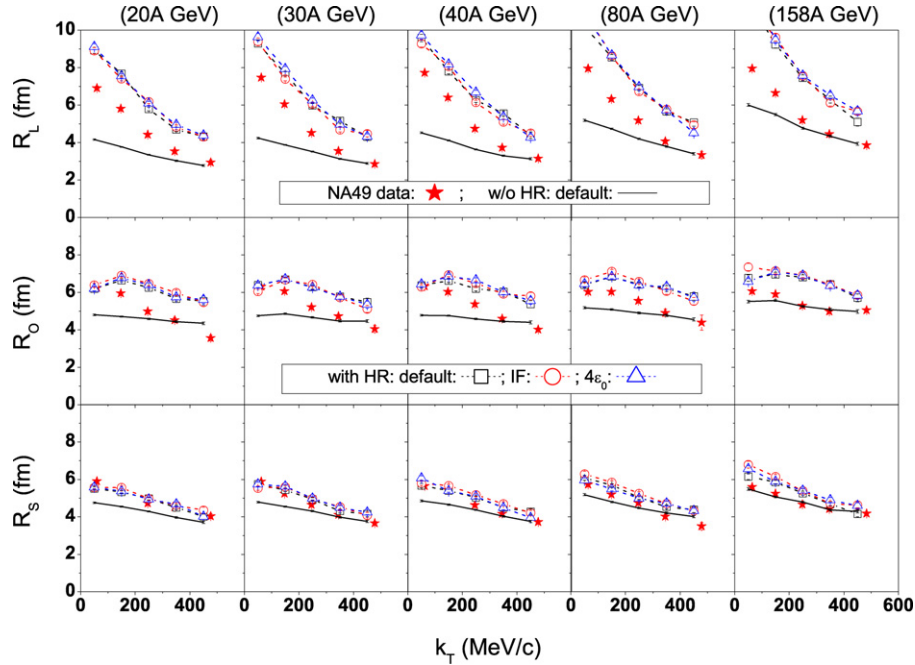
Fig. 4. k_T dependence of the HBT radii R_L, R_O, and R_S (at midrapidity) for central HICs at SPS energies ($E_{lab} = 20A$, $30A$, $40A$, $80A$, and $158A$ GeV). The NA49 data are indicated by solid stars [48]. The HG-EoS is employed in all calculations but under different freeze-out conditions: (1) without HR, calculations with default hydro-freeze-out criteria (GF, $5 \cdot \varepsilon_0$) are depicted by lines. (2) full hybrid model calculations with two different cuts of the energy density (default and $4 \cdot \varepsilon_0$) for the GF and with the default cut of the energy density for the IF are depicted by dashed lines with symbols.

should be able to fly into the detector without being forced into the hydrodynamic evolution.

Fig. 4 illustrates the k_T dependence of the HBT radii under various freeze-out conditions, which may be divided into two parts: (1) without HR and (2) with HR after the hydrodynamic phase. Here, without HR (lines) means that the evolution is stopped immediately after the Cooper–Frye freeze-out from the hydrodynamic phase (GF and $5 \cdot \varepsilon_0$ are adopted as default hydro-freeze-out criteria), with instantaneous resonance decays. The observed size of the pion source is small at this hydrodynamic freeze-out. In previous investigations [21] it has been found that binary baryon–meson and meson–meson collisions still frequently happen after the hydrodynamic freeze-out. In baryon–meson reactions, the most abundant interactions are the excitation and the decay of the Δ resonance (i.e. $\Delta \rightleftharpoons \pi N$), while in meson–meson collisions, the $\rho \rightleftharpoons \pi \pi$ process is dominant. A large number of these final hadron interactions in which pions are involved contribute significantly to the final HBT radii of pions in this model.

Let us therefore explore if the finally observed HBT radii do depend on the transition criterion from hydrodynamics to the transport model. The full hybrid model calculations (dashed lines with open symbols) are shown with two different cuts of the energy density ($5 \cdot \varepsilon_0$ as default and $4 \cdot \varepsilon_0$) for the GF and with the energy density cut $5 \cdot \varepsilon_0$ for the IF. It is found that the final state hadronic interactions are sufficient that the effects of different treatments of the hydrodynamic freeze-out on the final HBT radii are almost totally washed out in all directions and at all investigated energies.

Let us finally explore the dependence of the R_O/R_S ratio on the different EoS and freeze-out prescriptions. This ratio was expected to be sensitive to the duration time of the homogeneity region. In Fig. 5 the excitation function of the R_O/R_S ratio with the different EoS (lines with solid symbols) and freeze-out prescriptions (dashed lines with open symbols) are shown. The k_T bin 200–300 MeV/c is chosen. The result for the pure cascade calculation is also shown as a baseline (dotted line). It is seen clearly that the R_O/R_S ratio is sensitive to the EoS, but not to the various hydrodynamic freeze-out prescriptions when including HR (shown as open trian-
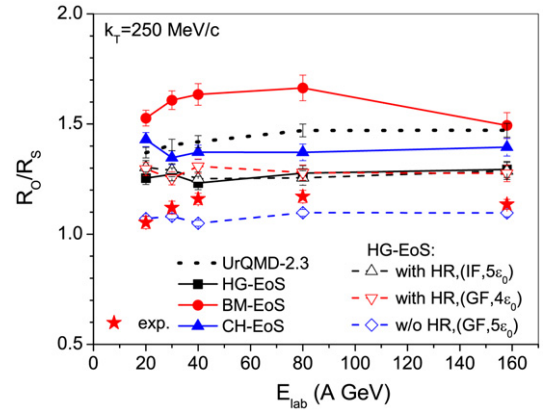

Fig. 5. Excitation function of the R_O/R_S ratio at $k_T = 250$ MeV/c. The NA49 data are indicated by solid stars [48]. UrQMD cascade calculation is shown by dotted line. Hybrid model calculations with EoS of HG, BM, and CH and with HR are shown by lines with solid symbols (the default hydro-freeze-out criteria (GF, $5 \cdot \varepsilon_0$) are used). In the HG-EoS mode, various criteria of freeze-out, (IF, $5 \cdot \varepsilon_0$) and (GF, $4 \cdot \varepsilon_0$) with HR, and the default (GF, $5 \cdot \varepsilon_0$) without HR are shown by dashed lines with open symbols.

gles and open inverted triangles) as it has already been implied from the results of the HBT radii shown in Figs. 2 and 4. With increasing latent heat which corresponds to the softness of EoS implied from Fig. 1, the R_O/R_S ratio is increased. The "excessively" large latent heat in BM-EoS results in a long duration time of the pion source and hence a large R_O/R_S ratio. Although the overall height is largely overpredicted by the BM-EoS, the qualitative behavior of the data (with a maximal lifetime at beam energies around 40–100A GeV) is well reproduced. In addition, the "peak structure" is less pronounced than in previous predictions [11], due to the different initial state and seems to provide a more reasonable estimate of the magnitude of the lifetime enhancement. The chiral EoS CH exhibits a lower R_O/R_S ratio because the first-order phase transition is less pronounced. The calculation with HG mode

(line with solid squares) leads to the smallest R_O/R_S ratio due to the most stiffest EoS among the three ones. The result of the cascade calculation lies in between the CH and the BM modes, which implies a relatively soft EoS. It can be understood since in the pure UrQMD model the new particle production is treated either as a resonance decay or a fragmentation of the string, which introduces a finite lifetime and hence leads to a softer EoS. After considering the mean field potentials for both confined and "pre-formed" particles [13,25], which gives a strong repulsion at the early stage, the R_O/R_S ratio was seen to decrease in line with results obtained here.

For the full hybrid model calculation the different freeze-out prescriptions do not affect the final results (when comparing the results by dashed lines with open triangles with that by the line with solid squares). The calculation with HG-EoS but without HR (dashed line with open diamonds) seems to provide better description of the data, but, seems clearly unphysical to the authors as a solution to the duration time problem.

5. Summary and outlook

In summary, the HBT correlation of the negatively charged pion source created in central Pb + Pb collisions at SPS energies was investigated with a hybrid model that incorporates a $(3 + 1)$d hydrodynamic evolution in the UrQMD transport approach. We explored different settings, one where the EoS was varied without changing the initial conditions and the freeze-out prescription and another where the EoS was fixed and the treatment of the freeze-out was changed. We presented a systematic investigation of these effects on the HBT radii. It was found that the latent heat influences the emission of particles visibly and hence the HBT radii of the pion source. While the final rescatterings result in an independence of the calculated HBT-parameters from the transition criterion, they do not improve the quantitative agreement with the experimental data. The details of the hydro-freeze-out prescription do not affect the HBT radii as well as the R_O/R_S ratio as long as the HR in the subsequent hadronic transport model were taken into account. Overall, the HBT data seem to favor a stiff EoS [51], but one should also keep in mind that viscosity effects are neglected during the hydrodynamic stage and that the particle emission from the early stages should be handled more carefully.

In the future, bulk and shear viscosity will be further considered for the hydrodynamic phase, and the non-equilibrated particle emission should be treated more precisely.

Acknowledgements

References

[1] D.H. Rischke, Y. Pursun, J.A. Maruhn, Nucl. Phys. A 595 (1995) 383;
    D.H. Rischke, Y. Pursun, J.A. Maruhn, Nucl. Phys. A 596 (1996) 717, Erratum.
[2] C. Spieles, H. Stöcker, C. Greiner, Phys. Rev. C 57 (1998) 908.
[3] M. Bluhm, B. Kampfer, R. Schulze, D. Seipt, U. Heinz, Phys. Rev. C 76 (2007) 034901.
[4] Z. Fodor, S.D. Katz, JHEP 0203 (2002) 014.
[5] P. de Forcrand, O. Philipsen, JHEP 0701 (2007) 077.
[6] S.V. Afanasiev, et al., NA49 Collaboration, Phys. Rev. C 66 (2002) 054902.
[7] C. Alt, et al., NA49 Collaboration, Phys. Rev. C 77 (2008) 024903.
[8] P.F. Kolb, P. Huovinen, U.W. Heinz, H. Heiselberg, Phys. Lett. B 500 (2001) 232.
[9] M. Bleicher, H. Stöcker, Phys. Lett. B 526 (2002) 309.
[10] H. Petersen, Q. Li, X. Zhu, M. Bleicher, Phys. Rev. C 74 (2006) 064908.
[11] D.H. Rischke, M. Gyulassy, Nucl. Phys. A 608 (1996) 479.
[12] D. Adamova, et al., CERES Collaboration, Phys. Rev. Lett. 90 (2003) 022301.
[13] Q. Li, M. Bleicher, H. Stöcker, Phys. Lett. B 659 (2008) 525.
[14] S. Pratt, J. Vredevoogd, Phys. Rev. C 78 (2008) 054906.
[15] M.A. Lisa, S. Pratt, arXiv:0811.1352 [nucl-ex].
[16] W. Broniowski, M. Chojnacki, W. Florkowski, A. Kisiel, Phys. Rev. Lett. 101 (2008) 022301.
[17] R. Andrade, F. Grassi, Y. Hama, T. Kodama, O.J. Socolowski, Phys. Rev. Lett. 97 (2006) 202302.
[18] T. Hirano, U.W. Heinz, D. Kharzeev, R. Lacey, Y. Nara, Phys. Lett. B 636 (2006) 299.
[19] C. Nonaka, S.A. Bass, Phys. Rev. C 75 (2007) 014902.
[20] J. Steinheimer, M. Bleicher, H. Petersen, S. Schramm, H. Stöcker, D. Zschiesche, Phys. Rev. C 77 (2008) 034901.
[21] H. Petersen, J. Steinheimer, G. Burau, M. Bleicher, H. Stöcker, Phys. Rev. C 78 (2008) 044901.
[22] Q. Li, M. Bleicher, H. Stöcker, Phys. Rev. C 73 (2006) 064908.
[23] Q. Li, M. Bleicher, X. Zhu, H. Stöcker, J. Phys. G 33 (2007) 537.
[24] Q. Li, M. Bleicher, H. Stöcker, J. Phys. G 34 (2007) 2037.
[25] Q. Li, M. Bleicher, H. Stöcker, Phys. Lett. B 663 (2008) 395.
[26] Q. Li, M. Bleicher, J. Phys. G 36 (2009) 015111.
[27] S. Soff, S.A. Bass, A. Dumitru, Phys. Rev. Lett. 86 (2001) 3981.
[28] D. Zschiesche, S. Schramm, H. Stöcker, W. Greiner, Phys. Rev. C 65 (2002) 064902.
[29] See, e.g., Figs. 15 and 16 in the review article: M.A. Lisa, S. Pratt, R. Soltz, U. Wiedemann, Annu. Rev. Nucl. Part. Sci. 55 (2005) 357.
[30] M. Luzum, J.G. Cramer, G.A. Miller, Phys. Rev. C 78 (2008) 054905.
[31] M. Bleicher, et al., Nucl. Phys. A 638 (1998) 391.
[32] B. Nilsson-Almqvist, E. Stenlund, Comput. Phys. Commun. 43 (1987) 387.
[33] B. Andersson, G. Gustafson, B. Nilsson-Almqvist, Nucl. Phys. B 281 (1987) 289.
[34] T. Sjostrand, Comput. Phys. Commun. 82 (1994) 74.
[35] S.A. Bass, et al., Prog. Part. Nucl. Phys. 41 (1998) 255.
[36] M. Bleicher, et al., J. Phys. G 25 (1999) 1859.
[37] S.A. Bass, et al., Phys. Rev. Lett. 81 (1998) 4092.
[38] L.V. Bravina, et al., J. Phys. G 25 (1999) 351, arXiv:nucl-th/9810036.
[39] L.V. Bravina, et al., Phys. Rev. C 78 (2008) 014907, arXiv:0804.1484 [hep-ph].
[40] D.H. Rischke, S. Bernard, J.A. Maruhn, Nucl. Phys. A 595 (1995) 346.
[41] D. Zschiesche, S. Schramm, J. Schaffner-Bielich, H. Stöcker, W. Greiner, Phys. Lett. B 547 (2002) 7.
[42] P. Papazoglou, D. Zschiesche, S. Schramm, J. Schaffner-Bielich, H. Stöcker, W. Greiner, Phys. Rev. C 59 (1999) 411.
[43] J. Theis, G. Graebner, G. Buchwald, J.A. Maruhn, W. Greiner, H. Stöcker, J. Polonyi, Phys. Rev. D 28 (1983) 2286.
[44] D. Zschiesche, G. Zeeb, S. Schramm, H. Stöcker, J. Phys. G 31 (2005) 935.
[45] D. Zschiesche, G. Zeeb, S. Schramm, J. Phys. G 34 (2007) 1665.
[46] S. Pratt, CRAB version 3, http://www.nscl.msu.edu/~pratt/freecodes/crab/home.html.
[47] http://root.cern.ch/.
[48] C. Alt, et al., NA49 Collaboration, Phys. Rev. C 77 (2008) 064908.
[49] F. Grassi, Y. Hama, T. Kodama, Phys. Lett. B 355 (1995) 9.
[50] J. Knoll, arXiv:0803.2343 [nucl-th].
[51] S. Bekele, et al., arXiv:0706.0537 [nucl-ex].